JOURNAL OF VIROLOGY, Oct. 2005, p. 12840–12851 Vol. 79, No. 20
0022-538X/05/$08.00+0 doi:10.1128/JVI.79.20.12840–12851.2005


# Identification and Functional Evaluation of Cellular and Viral Factors Involved in the Alteration of Nuclear Architecture during Herpes Simplex Virus 1 Infection

Martha Simpson-Holley,[1] Robert C. Colgrove,[1] Grzegorz Nalepa,[2] J. Wade Harper,[2] and David M. Knipe[1]*

*Departments of Microbiology and Molecular Genetics[1] and Pathology,[2] Harvard University Medical School, Boston, Massachusetts 02115*

Received 26 May 2005/Accepted 29 July 2005

**Herpes simplex virus 1 (HSV-1) replicates in the nucleus of host cells and radically alters nuclear architecture as part of its replication process. Replication compartments (RCs) form, and host chromatin is marginalized. Chromatin is later dispersed, and RCs spread past it to reach the nuclear edge. Using a lamin A-green fluorescent protein fusion, we provide direct evidence that the nuclear lamina is disrupted during HSV-1 infection and that the UL31 and UL34 proteins are required for this. We show nuclear expansion from 8 h to 24 h postinfection and place chromatin rearrangement and disruption of the lamina in the context of this global change in nuclear architecture. We show HSV-1-induced disruption of the localization of Cdc14B, a cellular protein and component of a putative nucleoskeleton. We also show that UL31 and UL34 are required for nuclear expansion. Studies with inhibitors of globular actin (G-actin) indicate that G-actin plays an essential role in nuclear expansion and chromatin dispersal but not in lamina alterations induced by HSV-1 infection. From analyses of HSV infections under various conditions, we conclude that nuclear expansion and chromatin dispersal are dispensable for optimal replication, while lamina rearrangement is associated with efficient replication.**

Herpes simplex virus 1 (HSV-1) forms replication compartments (RCs) in the infected cell nucleus (32), in which DNA replication, late viral transcription, and viral nucleocapsid assembly occur. In doing so, the virus causes cytopathic effects by affecting factors that control nuclear architecture: host cell chromatin and the nuclear lamina (5, 24, 34, 40, 41). During infection, RCs form from small prereplicative sites and expand into large globular domains, disrupting the nuclear interior by compressing and marginalizing host chromatin (24, 39, 44, 45). Following assembly, nucleocapsids are thought to exit the nucleus by budding at the inner nuclear membrane into the perinuclear space (11). This requires that nucleocapsids move through the host chromatin layer and the nuclear lamina to reach the membrane. Thus, HSV-1 manipulates the nuclear interior and periphery to achieve replication and egress.

Several studies have described changes in the nuclear lamina during infection with different herpesviruses (9, 25, 34, 40, 41). Mouse cytomegalovirus has been shown to disrupt the nuclear lamina, and two viral proteins, UL50 and UL53, have been implicated in this process (25). Homologues of these proteins appear to be present in several other viruses, including HSV-1, HSV-2, pseudorabies virus, and Epstein-Barr virus (EBV) (19, 21, 25, 35, 51). In EBV, the proteins BFLF2 and BFRF1 have been shown to interact and colocalize at the nuclear membrane, and BFRF1 binds to lamin B in vitro (9, 21). A mutant EBV lacking a functional BFRF1 gene is defective for replication in several cell lines and shows accumulation of nucleocapsids in the nucleus of infected cells (6). The homologous pseudorabies virus UL31 and UL34 proteins have been shown to interact with one another and are involved in nuclear egress, most likely through a role in primary envelopment (8, 19). In HSV-1, UL31 and UL34 have also been shown to be involved in nuclear egress. Mutant viruses lacking either the *UL31* or *UL34* open reading frame (ORF) show accumulation of nucleocapsids in the nucleus and have reduced titers when grown in noncomplementing cell lines (3, 38).

Previously we and others have shown that wild-type (wt) HSV-1 infection causes changes in the staining pattern of the nuclear lamina using antibodies to lamin A/C and lamina-associated protein 2 (LAP2) (41). The distribution of these proteins is discontinuous and punctate in HSV-1-infected cells, in contrast to the continuous nuclear lamina staining seen in uninfected cells. Cells infected with either the dUL31 or dUL34 virus do not show alterations in lamina staining with antibodies to lamin A/C or LAP2, implying that UL31 and UL34 are involved in disrupting the lamina (34, 41). However, there is evidence that UL31 binds to lamin A/C in vitro, and Reynolds et al. have postulated that this binding might cause epitope masking, leading to an artifactually altered distribution of lamin A/C in infected cells (34).

The mechanisms by which the UL31 and UL34 proteins act to promote nuclear egress are unclear. During infection, UL31 and UL34 localize to the nuclear rim (35, 36). UL31 has been shown to bind to lamin A in vitro (34). UL31 and UL34 also interact with one another, and US3 may also play a role in facilitating their activity at the nuclear periphery (22, 36). If the proteins do cause changes in lamina structure, it is not known how these changes are achieved. Thus, it is currently of importance to define the changes that occur at the nuclear periphery

* Corresponding author. Mailing address: Department of Microbiology and Molecular Genetics, Harvard Medical School, 200 Longwood Avenue, Boston, MA 02115. Phone: (617) 432-1934. Fax: (617) 432-0223. E-mail: david_knipe@hms.harvard.edu.

during HSV-1 infection and to resolve their role in altering nuclear architecture during infection and in promoting viral replication.

In addition to studies of the nuclear lamina, HSV-1 has been shown to alter host cell chromatin distribution and to cause an increase in nuclear size (24). RCs occupy the interchromosomal space, which expands at the expense of host chromatin; chromatin is compressed and marginalized to form a layer at the edge of the nucleus (24). We have shown that this host layer is eventually dispersed by viral infection as RCs expand through it to reach the nuclear periphery (41).

Nuclear size increases have previously been described at 8 h postinfection (hpi) and 9.5 hpi in HSV-1-infected HeLa cells (24). Nuclear expansion occurs alongside RC formation, chromatin compression, and displacement. The cellular mechanisms by which nuclear size is controlled are not well understood. In addition to chromatin and the nuclear lamina, factors potentially involved in the control of nuclear size include nuclear actin, the cytoskeleton, and a putative nucleoskeleton (1, 26, 43). In cell biological studies of uninfected cells, change in nuclear size is coupled to cytoplasmic size (43). During HSV-1 infection, nuclear size apparently becomes uncoupled from cytoplasmic size and nuclear expansion is observed in the face of cytoplasmic shrinkage and cell rounding (37).

Recently, evidence has accumulated supporting the existence of actin in the nucleus, with potential functions including chromatin remodeling, transcription, mRNA export, and nuclear structure and integrity (1, 31). Because nuclear actin cannot be stained by conventional chemical or immunological techniques, it is thought to adopt a different form from that of conventional cytoplasmic F-actin (1, 10, 31). Nuclear actin may exist as monomeric G-actin or may adopt a novel conformation. The lack of reagents available to study nuclear actin has made it difficult to establish its role in vivo. HSV-1 infection provides an opportunity to measure the impact of actin disruption on nuclear size in a system in which significant changes in nuclear size are induced by the virus.

The existence of a nucleoskeleton, and the function of such a structure, has been a controversial area of research (23, 26, 29, 30, 48). Previous techniques used to isolate the nuclear matrix have revealed a network of material which has been postulated by some to be functionally equivalent to a nucleoskeleton and by others to be an artifactual residue of nuclear components (23, 30). No identification of such a network was possible in living cells until a recent study described the localization of a cellular protein phosphatase, Cdc14B (26). Cdc14B is a homologue of the *Saccharomyces cerevisiae* protein Cdc14p, which is crucial for cell cycle progression (46). Both endogenous Cdc14B and a green fluorescent protein (GFP)-Cdc14B fusion protein adopt a nuclear distribution and form a network that radiates from nucleoli to the nuclear membrane. GFP-Cdc14B is visible as part of such a network in both fixed and living cells. Thus, evidence now exists for a nucleoskeleton in living cells. However, the functional role of this nucleoskeleton and the potential involvement of the nucleoskeleton in viral replication are so far undefined.

Here, we present findings relating to the effects of HSV-1 infection on nuclear architecture and the impact of these changes on viral replication. We investigate the role of viral and cellular factors in these changes.

## MATERIALS AND METHODS

**Cells and viruses.** RD14 cells containing the *UL31* gene (3) were the kind gift of Bernard Roizman. 143/1099E cells containing the *UL34* gene (38) were the gift of Richard Roller. RD14, 143/1099E, HEp-2, U2OS, and Vero cells were maintained in Dulbecco's modified Eagle's medium (DMEM, Gibco-BRL) supplemented with 5% heat-inactivated fetal calf serum (FCS) and 5% heat-inactivated newborn calf serum.

The R5132 deletion mutant virus lacking the *UL31* gene and the rescued virus R5133 (3) were the kind gifts of Bernard Roizman. The RR1072 mutant virus lacking the *UL34* gene and the rescued virus RR1072R (38) were the gifts of Richard Roller. For preparation of viral stocks, viruses were grown in the appropriate complementing cell lines (the KOS strain was grown in Vero cells). Titers were determined by plaque assay in Vero cells or the appropriate complementing cell line. Viral titrations were performed as previously described (41).

For single-cycle growth curve experiments, wild-type, mutant, and rescued viruses were used to infect Vero cells at a multiplicity of infection (MOI) of 10. At 1 hpi, cells were washed with an acid wash buffer (135 mM NaCl, 10 mM KCl, 40 mM citric acid, pH 3) three times for 30 seconds and then washed twice with DMEM before incubation at 37°C in DMEM plus 1% FCS for the appropriate time periods. Total viral yields were determined by plaque assay as described previously (41) on the appropriate complementing cell line or on Vero cells for wild-type HSV-1.

For infection experiments, viruses were used at an MOI of 10 to infect HEp-2 cells, which were incubated at 37°C for 1 h before removal of the inoculum and addition of DMEM supplemented with 1% FCS. For infection of previously transfected cells, an MOI of 50 was used.

**Drug treatment.** Cytochalasin D (CD; Sigma) and latrunculin A (LA; Molecular Probes) were dissolved in dimethyl sulfoxide (DMSO). Dilutions were done in DMEM plus 1% FCS and used to treat HEp-2 cells following infection with wt HSV-1 strain KOS at an MOI of 20 for 2 h at 37°C. The inoculum was removed before the addition of drug-containing medium. As a solvent control, DMSO was added to DMEM plus 1% FCS, the amount of DMSO added in each experiment being equal to the largest volume of drug solution used. Cytochalasin D was used at a concentration of 2 μM, and latrunculin A was used at a concentration of 1 μM. Similar results were observed using both drugs across a range of 1 to 3 μM (data not shown).

**Plasmids and transfections.** Plasmid pGFPWTLA, expressing a GFP-lamin A fusion protein, was kindly provided by D. M. Gilbert (18). Plasmid pGFPCdc14B has been described previously (26). The day before transfection, HEp-2 or U2OS cells were seeded into 24-well plates containing glass coverslips for fluorescence experiments. Transfections were carried out using Lipofectamine reagent (Gibco-BRL) according to the manufacturer's instructions, except for transfection of pGFPCdc14B, which was done using Fugene reagent (Roche). Cells were fixed for immunofluorescence following infection or mock infection.

**Antibodies and immunofluorescence.** Antibodies to UL31 and UL34 have been described elsewhere (35). Mouse monoclonal antibody to lamin A/C was obtained from Santa Cruz Biotechnology Inc. Mouse monoclonal antibody to LAP2 was obtained from BD Transduction Technologies. Antibody to histone H1 was obtained from Upstate Biotechnology Inc. The 3-83 antiserum specific for ICP8 has been described elsewhere (20). Tetramethyl rhodamine isocyanate (TRITC)-labeled phalloidin was obtained from Sigma. Secondary antibodies conjugated to Alexa 594 and Alexa 488 dyes were obtained from Molecular Probes Inc.

HEp-2 cells were seeded for immunofluorescence at $2 \times 10^5$ cells/well on glass coverslips in 24-well plates and incubated overnight at 37°C before infection or transfection. Following incubation for the appropriate time, cells were fixed in 4% formaldehyde in phosphate-buffered saline (PBS) for 20 min at room temperature. Cells were permeabilized in acetone at −20°C for 2 min. Following several washes in PBS, cells were blocked overnight in IF buffer (PBS containing 4% goat serum [Sigma]). Primary antibodies were diluted appropriately and applied to cells in IF buffer, and the cells were incubated for 1 h at room temperature. Lamin A/C antibody was used at 1:10, LAP2 at 1:200, H1 at 1:200, and 3-83 at 1:200. Cells were washed three times for 5 min in IF buffer. Secondary antibodies were applied at 1:1,000 in IF buffer for 30 min at room temperature. Cells were then washed three times for 5 min in IF buffer at room temperature, and coverslips were mounted with Prolong antifade reagent (Molecular Probes, Inc.).

Slides were viewed with an Axioplan 2 microscope (Zeiss) with a 63× objective and a 10× ocular objective. Images were collected with the Axiovision 5.2 suite of programs (Zeiss) and a Hamamatsu C4742-95-12NR digital camera. Nuclear cross-sectional areas were measured using the Axiovision 5.2 program. Signifi-

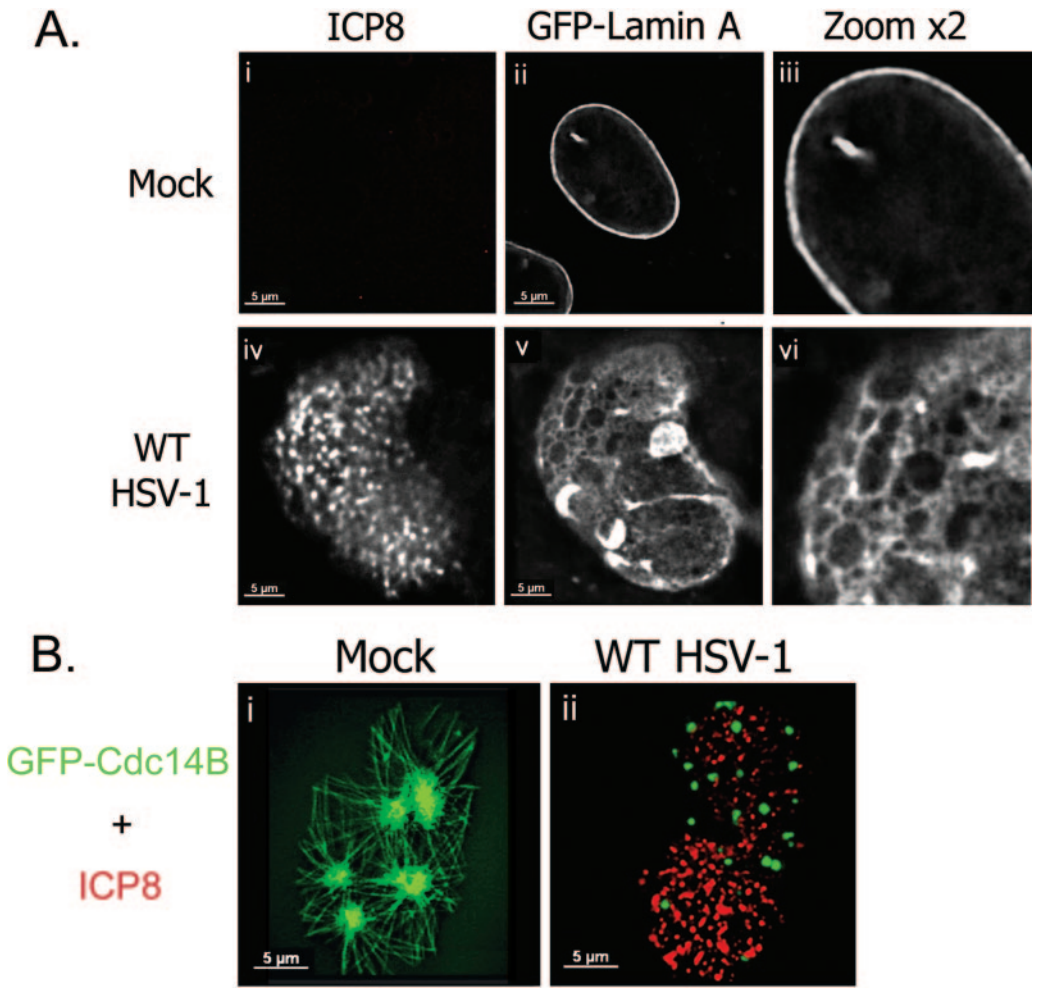


FIG. 1. Effects of HSV-1 infection on the nuclear lamina and nucleoskeleton. (A) Digital fluorescence micrographs of HEp-2 cells transfected with pGFPLaminA and either mock infected (i to iii) or infected with wt HSV-1 (iv to vi). Cells were fixed at 16 hpi and stained with antibody to ICP8 (i and iv). Single-channel images are shown (i to iii and iv to vi). To show detail, areas of each image were enlarged by a factor of two (iii and vi). (B) Digital fluorescence micrographs of U2OS cells transfected with pGFPCdc14B and either mock infected (i) or infected with wt HSV-1 (ii). Cells were fixed at 16 hpi and stained with antibody to ICP8 (red). Merged-channel images are shown.

cance testing for differences in nuclear cross-sectional area was done using the Wilcoxon rank test for nonnormal samples with Bonferroni correction for multiple comparisons applied where appropriate. Box and whisker plots were drawn to show the median, 95% confidence interval, first and third quartiles, and data range for each experimental condition. For each group, $n$ was 20 to 23. Statistical calculations were carried out using the open-source R package of statistical software (http://www.r-project.org/). Fluorescence images were compiled into montages with Adobe Photoshop, and close-up digital enlargements were obtained using the same program. All images are to scale.

**SDS-PAGE and Western blotting.** HEp-2 cells were infected with HSV-1 strain KOS at an MOI of 10 and treated with LA or CD at 2 hpi. At 16 hpi, cells were harvested in Laemmli's sample buffer and samples were immediately incubated in a boiling water bath for 5 min. Proteins were separated by sodium dodecyl sulfate-polyacrylamide gel electrophoresis (SDS-PAGE) and electrically transferred to a polyvinylidene difluoride membrane with the Bio-Rad Transblot system according to the manufacturer's instructions. Membranes were probed with antisera to UL31 (1:200) or UL34 (1:200), washed three times for 5 min in PBS plus 0.2% Tween 20 (Sigma), and incubated with secondary antibodies conjugated to horseradish peroxidase diluted 1:10,000. Horseradish peroxidase signal was detected using chemiluminescence reagents (ECL; Amersham) exposed on standard X-ray film (Kodak).

## RESULTS

**HSV-1 infection causes the redistribution of a GFP-lamin A fusion protein.** Previous studies have shown discontinuities in the nuclear lamina during HSV-1 infection using antibodies to lamin A/C and LAP2 (34, 41). However, it has been suggested that the apparent change in localization of lamin A/C might be due to epitope masking (34). Thus, we used an antibody-independent method to visualize a GFP-lamin A fusion protein and look for changes in its distribution during HSV-1 infection. We transfected a plasmid expressing GFP-lamin A into HEp-2 cells, which were then infected or mock infected with wt HSV-1 and incubated for 16 h. Following fixation, cells were stained with an antibody to ICP8 as a marker of infection.

In mock-infected cells, the GFP-lamin A protein was incorporated specifically into the nuclear lamina, forming a smooth continuous layer (Fig. 1A, i to iii). This has been previously reported using this construct (18). Nuclei were of a uniform size and shape (Fig. 1A, ii and iii). No staining was observed using the ICP8 antibody (Fig. 1A, i). In cells infected with wt HSV-1, large RCs were observed using antibody to ICP8. In such cells, the localization of GFP-lamin A was altered (Fig. 1A, iv to vi). Nuclear size increased, and nuclei were irregular in shape. The GFP-lamin A layer was fenestrated, and hernia-

tions were observed which contained GFP-lamin A protein (Fig. 1A, v and vi). This was seen in most cells containing RCs following infection for 16 h but was not observed before 10 hpi (data not shown). These results show definitively that the nuclear lamina is rearranged and perforated during HSV-1 infection.

**HSV-1 infection disrupts a nucleoskeletal structure in the nuclear interior.** A recent report has shown that the cellular protein Cdc14B is incorporated into an intranuclear network in living and fixed cells (26). To examine the effect of HSV-1 infection on this network, we transfected U2OS cells with a plasmid expressing GFP-Cdc14B and infected or mock infected them with HSV-1. Cells were then fixed and stained with antibodies to ICP8. Consistent with published results (26), mock-infected cells showed a network of GFP-Cdc14B which radiated from nucleoli to the nuclear edge (Fig. 1B, i). Such networks were visible in around 80% of GFP-Cdc14B-expressing cells, the remainder showing a predominantly nucleolar localization (data not shown). In the presence of HSV-1 infection, the distribution of GFP-Cdc14B was dramatically altered (Fig. 1B, ii). Instead of forming nucleoskeletal structures, GFP-Cdc14B was observed in punctate structures distributed throughout the nucleus. Infected cells were counted and scored for GFP-Cdc14B distribution, and 90% of infected cells showed relocalization to punctate nuclear structures (data not shown). RCs did not seem to exclude the GFP-Cdc14B accumulations, but ICP8 did not colocalize with GFP-Cdc14B. GFP-Cdc14B did not appear to be specifically localized to any nuclear compartment. Very similar rearrangement of GFP-Cdc14B was observed in HSV-1-infected HEp-2 cells (data not shown). Thus, infection with wt HSV-1 disrupted a preexisting nucleoskeletal structure labeled by GFP-Cdc14B and induced the dramatic rearrangement of this cellular protein.

**HSV-1 infection causes significant nuclear expansion, concurrent with RC maturation and viral replication.** To address the relevance of the time points used in the context of viral replication, we examined the time course of virus production. HEp-2 cells were infected with HSV-1, and total viral yield was measured by plaque assay at various time points. In multiple experiments, viral yield was observed to increase from 2 h to 24 hpi (Fig. 2C and data not shown). At 16 hpi, the rate of infectious virus production was similar to that observed at 8 hpi. Thus, the 16-hpi time point appears to be significant and representative of viral replication.

An increase in nuclear size during HSV-1 infection in other systems has been recorded previously (24). We investigated this further to define the changes occurring throughout infection and to correlate nuclear size changes with other observed changes in nuclear architecture. We infected HEp-2 cells with HSV-1, and at various times postinfection, cells were fixed and stained by immunofluorescence for viral (ICP8) and cellular (H1) proteins. To quantify nuclear expansion, cells were imaged using a fluorescence microscope and digital camera, and the widest focal *xy* plane of the nucleus was used to quantify the cross-sectional area. Nuclear volume was also calculated using the diameters of nuclei in three dimensions at each time point and applying the equation for the volume of an ellipsoid (data not shown). The trend shown by nuclear volume was in agreement with the data obtained for cross-sectional area using quantitative microscopy software; therefore, cross-sectional area (Fig. 2B) was taken to be representative of nuclear size.

Nuclei of cells infected with HSV-1 expanded from 8 h to 16 hpi during viral replication (Fig. 2A, i to vi, and 2B). Mock-infected nuclei were relatively uniform in size, were evenly stained with the H1 antibody, and showed no staining for ICP8 (Fig. 2A, i, and 2B). Nuclear size in infected cells at 6 hpi was similar to that of mock-infected nuclei (Fig. 2b). Small prereplicative sites were stained for ICP8 at 6 hpi, surrounded by H1 staining (Fig. 2A, ii). At 8 hpi, RCs had formed and occupied a large portion of the nucleus (Fig. 2A, iii). Host chromatin was marginalized and excluded from RCs, and at 8 hpi the average cross-sectional area showed a significant increase (Fig. 2B). By 10 hpi, some expansion of RCs had occurred, and many nuclei were noticeably larger than those observed earlier or in mock-infected samples (Fig. 2A, iv). Nuclei and RCs had expanded further by 12 hpi, and H1 staining showed marginalization of host chromatin to a thin intact layer at the nuclear boundary. As reported previously (41), maturation of RCs subsequently occurred, and by 16 hpi ICP8 staining extended through the chromatin layer to the edge of the nucleus (Fig. 2A, v and vi). At 16 hpi, the median area of infected nuclei was more than double the mock-infected value (16 hpi, 266 $\mu m^2$; mock, 129 $\mu m^2$). At 24 hpi, nuclei looked similar to those at the 16-hpi time point (data not shown), and the nuclear size observed at 16 hpi was maintained (Fig. 2B). No further expansion of the nucleus was observed after 16 hpi, following RC maturation (Fig. 2A and B). The range of nuclear cross-sectional areas was also found to increase during infection with HSV-1. Mock-infected nuclei varied in cross-sectional area across a range of 63 $\mu m^2$. The range across which nuclear area varied increased throughout infection, reaching a maximum of 284 $\mu m^2$ at 16 hpi. At 24 hpi, the variation in cross-sectional area was reduced to a level similar to the range observed at 6 hpi. Thus, the introduction of virus to this experimental system increased nuclear cross-sectional area to a statistically significant degree and also increased variation in nuclear size.

**Viral factors involved in nuclear changes during infection with HSV-1. (i) The viral UL31 and UL34 proteins are necessary for rearrangement of the nuclear lamina.** Having observed certain changes in nuclear architecture caused by viral infection, we next did experiments to deduce the role of viral proteins in these processes. We looked at the requirement for the UL31 and UL34 viral proteins in the rearrangement of the GFP-lamin A fusion protein. HEp-2 cells were transfected with a plasmid expressing GFP-lamin A and were infected with wt HSV-1 or the mutant virus dUL31 or dUL34. At 16 hpi, cells were fixed and stained with an antibody to ICP8.

In cells infected with either of the mutant viruses dUL31 and dUL34, the GFP-lamin A distribution resembled that of mock-infected samples (Fig. 1A, ii and iii), showing a smooth continuous layer of GFP-lamin A protein at the nuclear periphery (Fig. 3A, iv and vi). Thus, deletion of either *UL31* or *UL34* from the viral genome prevented rearrangement of the GFP-lamin A fusion protein, as seen during wild-type infection (Fig. 3A, i and ii, and Fig. 1A). In further experiments in which the UL31, UL34, and GFP-lamin A proteins were coexpressed from plasmids in the absence of infection, the GFP-lamin A protein was rearranged in a manner similar to that described here during wild-type HSV-1 infection (data not shown). Thus,

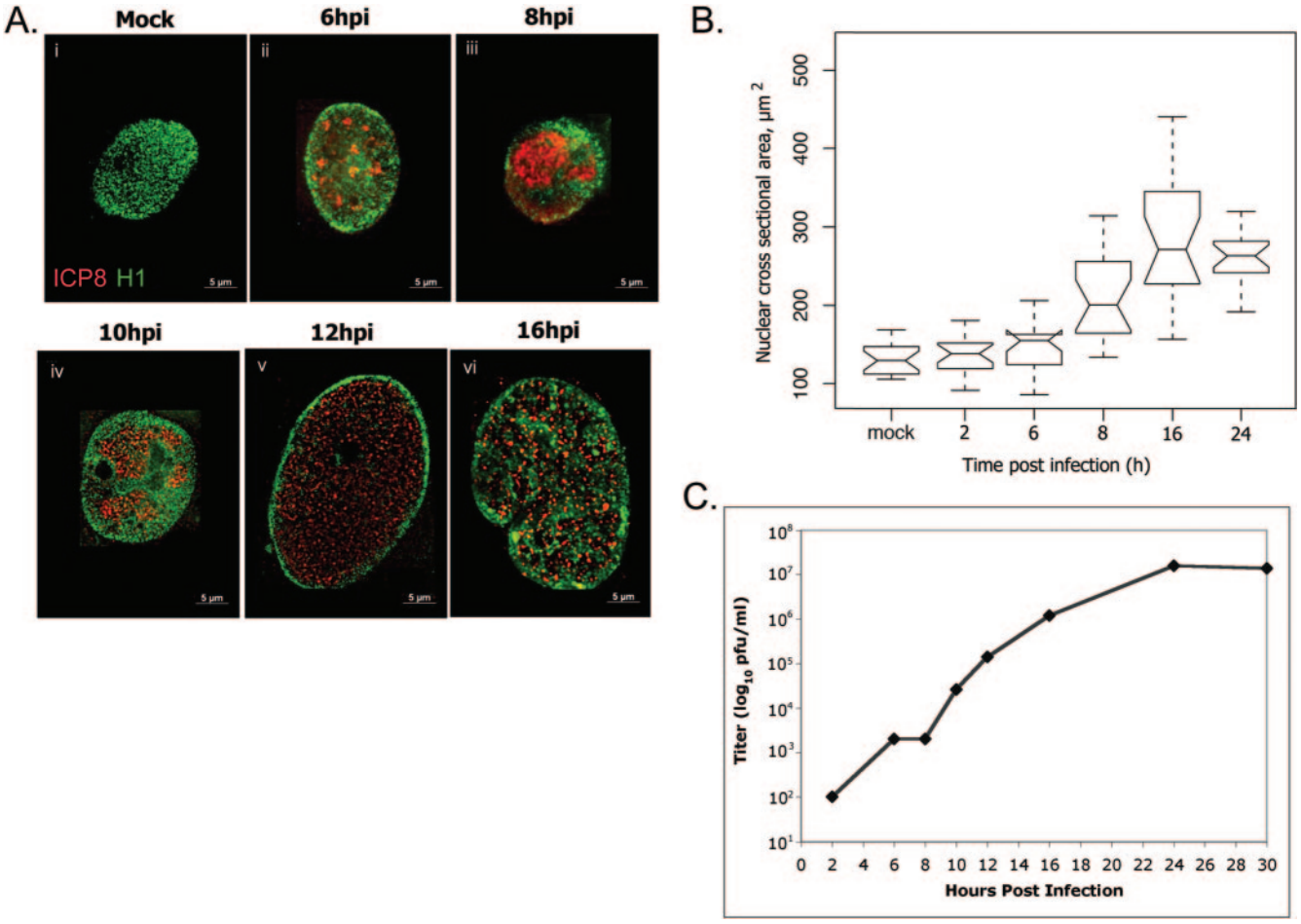


FIG. 2. Replication compartment formation and cell size change. (A) Digital images of fluorescence micrographs of HEp-2 cells mock infected (i) or infected with wt HSV-1 (ii to vi). Cells were stained for ICP8 (red) and histone 1 (H1, green). Merged-channel images are shown to scale. (B) Box and whisker plot showing statistical analysis of nuclear cross-sectional areas at times following infection (2, 6, 8, 16, and 24 h) or mock infection (mock) with wt HSV-1. Cells were stained with antibodies to ICP8 and H1, and nuclear cross-sectional areas were measured using microscopy software (Zeiss Axiovision 5.2). Lines at top and bottom show data ranges, excluding outliers. Open boxes show first and third quartiles. Notches show 95% confidence intervals for medians, shown as the central horizontal line in each box. (C) Graph showing viral yields at points during a single cycle of viral replication. HEp-2 cells were infected with wt HSV-1, and total infectivity at different times was measured by plaque assay on Vero cells. Graph shows a representative example of replicate experiments.

UL31 and UL34 are necessary and sufficient for lamina rearrangement.

**(ii) *UL31* and *UL34* are necessary for nuclear expansion during HSV-1 infection.** Previously, we have shown that mutants lacking *UL31* and *UL34* are unable to induce lamina rearrangement, chromatin fragmentation, and RC maturation (41). To quantify the effects of the dUL31 and dUL34 mutant viruses on nuclear size, nuclear cross-sectional areas were measured in HEp-2 cells either mock infected or infected with wt HSV-1, dUL31, or dUL34. Nuclei of cells infected with the mutant viruses had median cross-sectional areas that were very similar to those of mock-infected cell nuclei (Fig. 3B, mock, 130 $\mu m^2$; dUL31, 135 $\mu m^2$; dUL34, 136 $\mu m^2$). In contrast, nuclei of cells infected with the wild-type virus showed a significant increase in nuclear size, as described above (266 $\mu m^2$). Thus, in contrast to the wild-type virus in this system, the mutant viruses failed to cause increases in nuclear size and in variation of nuclear size.

**Cellular factors involved in HSV-1-induced nuclear changes. (i) Role of G-actin in changes to the nuclear interior during infection with HSV-1.** The existence of actin in the nucleus in a functional capacity is now widely accepted, but its potential role in HSV-1 infection has not yet been addressed. Therefore, we investigated a potential role for nuclear actin in the control of nuclear size during infection, using a system in which G-actin, the monomeric form of actin proposed to exist in the nucleus (31), could be disrupted.

HEp-2 cells were infected or mock infected with HSV-1 and treated with either LA to disrupt G-actin functions, CD to disrupt F-actin, or DMSO as a solvent control at 2 hpi. Cells were fixed at 16 hpi and stained using antibodies to ICP8 and either H1 or TRITC-phalloidin to detect the actin cytoskeleton. The effects of these treatments on cells were then studied using fluorescence microscopy.

In mock-infected cells, no significant alteration of nuclear structure or size by DMSO, CD, or LA was apparent (Fig. 4A,

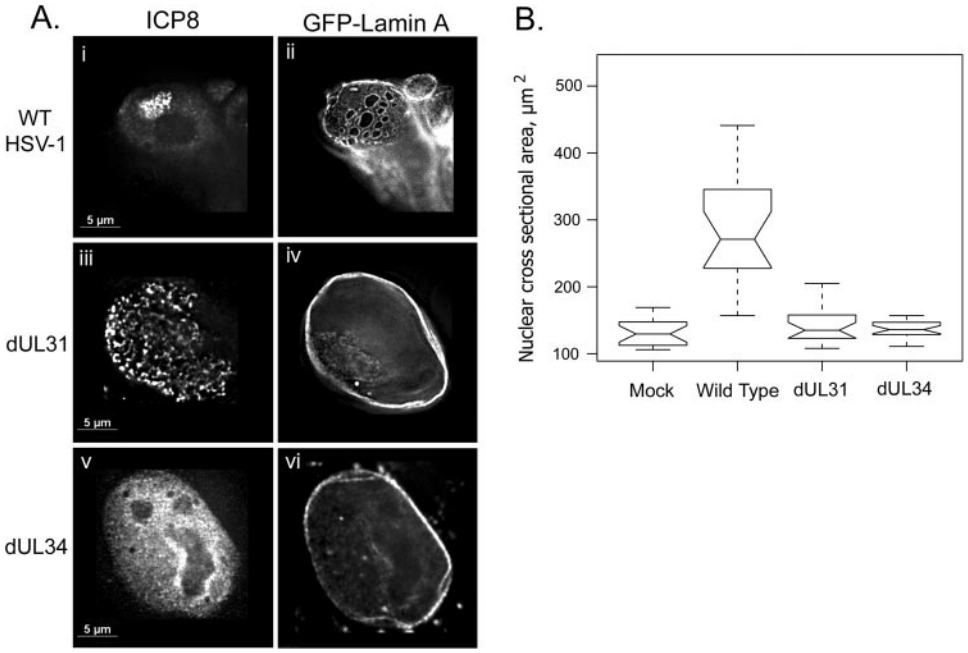


FIG. 3. Role of UL31 and UL34 in GFP-lamin redistribution and cell size change. (A) Digital images of fluorescence micrographs of HEp-2 cells transfected with pGFPLamin A and infected the next day with wt HSV-1 (i and ii) or the mutant virus dUL31 (iii and iv) or dUL34 (v and vi). Cells were fixed 16 hpi and stained with antibody to ICP8 (i, iii, and v). (B) Box and whisker plot of nuclear cross-sectional areas of HEp-2 cells mock infected (mock) or infected with wt HSV-1, dUL31, or dUL34 for 16 h. Cells were fixed and stained with antibodies to H1 and ICP8, and nuclear cross-sectional areas were measured using microscopy software (Zeiss Axiovision 5.2). Upper and lower bars represent limits of the data range. Open boxes represent first and third quartiles, with notches showing the 95% confidence interval for the median, which is shown as the central horizontal bar in each box.

v, vi, and vii). H1 staining showed an even distribution of this protein throughout the nucleus in both the presence and absence of the drugs, barring the nucleolus. Infected cells treated with DMSO showed a nuclear morphology similar to that described in untreated infected cells (Fig. 4A, i). In cells treated with CD, the effects were similar to those of the control infection, i.e., chromatin was marginalized and dispersed and RCs extended to the nuclear edge (Fig. 4A, ii). In contrast, LA treatment of cells had a striking effect on the nuclear changes induced by infection. RCs were observed to form in the center of the nucleus but did not extend to the nuclear edge (Fig. 4A, iii). Chromatin was marginalized but was not dispersed. Thus, G-actin disruption prevented certain HSV-1-induced changes in nuclear architecture.

To determine the effects of these drugs on the actin cytoskeleton, staining of cells with labeled phalloidin and anti-ICP8 was done (Fig. 4A, ix to xii). In DMSO-treated cells infected with HSV-1, replication compartments were evident by ICP8 staining. The actin cytoskeleton in such cells was similar to that observed in mock-infected cells (data not shown), showing smooth F-actin filaments stretching the length of the cell and lining the plasma membrane (Fig. 4A, ix). In cells treated with CD, no F-actin filaments were evident. Instead, actin was distributed in dense accumulations in the cytoplasm and underlying the plasma membrane (Fig. 4A, x). Actin staining in cells treated with LA was similar to that of CD-treated cells: actin was distributed in cytoplasmic accumulations and was aggregated underneath the plasma membrane (Fig. 4A, xi). Mock-infected cells treated with CD (data not shown) or LA (Fig. 4A, xii) resembled infected drug-treated cells: no F-actin filaments were observed and actin was present in accumulations. Cell rounding was evident in cells treated with either CD or LA (Fig. 4A, x to xii).

Nuclear size was evaluated in cells treated as described above, by measurement of nuclear cross-sectional area. In the presence of DMSO, wt HSV-1 caused significant nuclear expansion compared to mock-infected samples (Fig. 4B, HSV-1 median, 222 $\mu m^2$; mock median, 103 $\mu m^2$). The infected-cell median was more than double that of the mock-infected DMSO-treated sample, as seen above in untreated samples (Fig. 2A). The range across which nuclear size varied also increased in the presence of HSV-1, from 96 $\mu m^2$ in the mock-infected sample to 245 $\mu m^2$ in the HSV-1-infected sample. In the presence of CD, the median nuclear cross section was similar to that of the DMSO-treated sample, indicating that CD treatment did not prevent the nuclear size increase caused by HSV-1 infection (Fig. 4B, CD-treated median, 199 $\mu m^2$; DMSO-treated median, 222 $\mu m^2$).

In LA-treated cells, the effect of infection on nuclear size was very different from that in CD- or DMSO-treated cells. The median nuclear cross-sectional area of cells treated with LA was significantly smaller than that observed in DMSO-treated or CD-treated samples (Fig. 4B, LA, 120 $\mu m^2$; DMSO, 222 $\mu m^2$). The LA-treated sample showed no statistically significant increase in area over the mock-infected DMSO-treated sample (LA, 120 $\mu m^2$; mock DMSO, 103 $\mu m^2$). Thus, LA treatment prevented the HSV-1-induced increase in nuclear size recorded in the presence of DMSO or CD. Disrup-

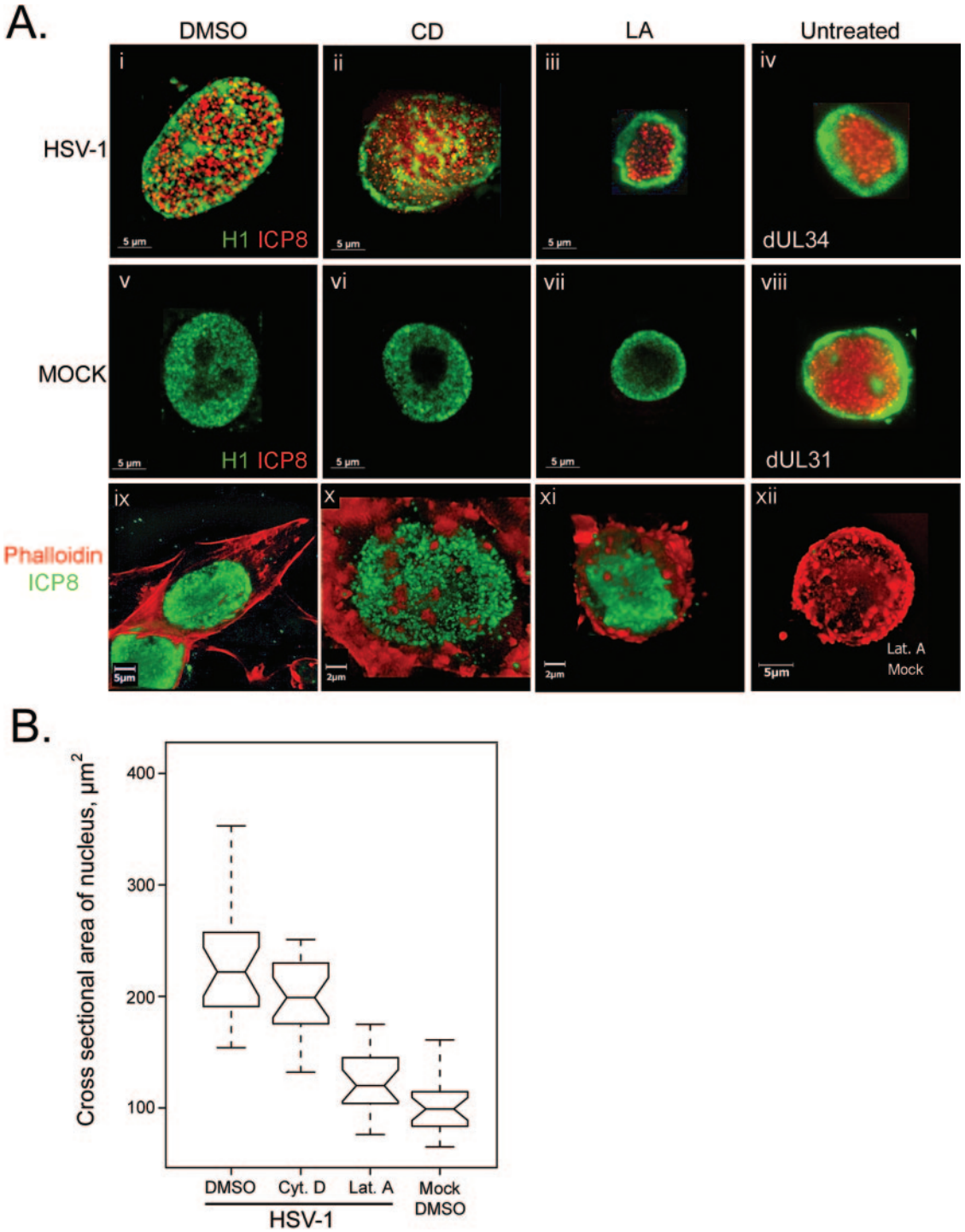


FIG. 4. Role of G- and F-actin in nuclear changes. (A) Digital images of fluorescence micrographs of HEp-2 cells mock infected (v to vii and xii) or infected with wt HSV-1 (i to iii and ix to xi) or the mutant virus dUL34 (iv) or dUL31 (viii). Cells infected or mock infected with wt HSV-1 were treated with DMSO (i, v, and ix), CD (ii, vii, and x), or LA (iii, vii, xi, and xii). Cells were fixed 16 hpi and stained using antibodies to H1 (green, i to viii) and ICP8 (red, i to viii) or with ICP8 (green, ix to xii) and TRITC-phalloidin (red, ix to xii). (B) Box and whisker plot showing nuclear cross-sectional areas of HEp-2 cells mock infected and treated with DMSO (Mock DMSO) or infected with wt HSV-1 and treated with DMSO, cytochalasin D (Cyt. D), or latrunculin A (Lat. A). Cells were fixed 16 hpi and stained with antibodies to H1 and ICP8. Nuclear cross-sectional areas were measured using microscopy software (Zeiss Axiovision 5.2). Upper and lower bars show the data range for each sample. Open boxes show first and third quartiles. Notches show the 95% confidence interval for each median value, which is represented by the central horizontal bar in each box.

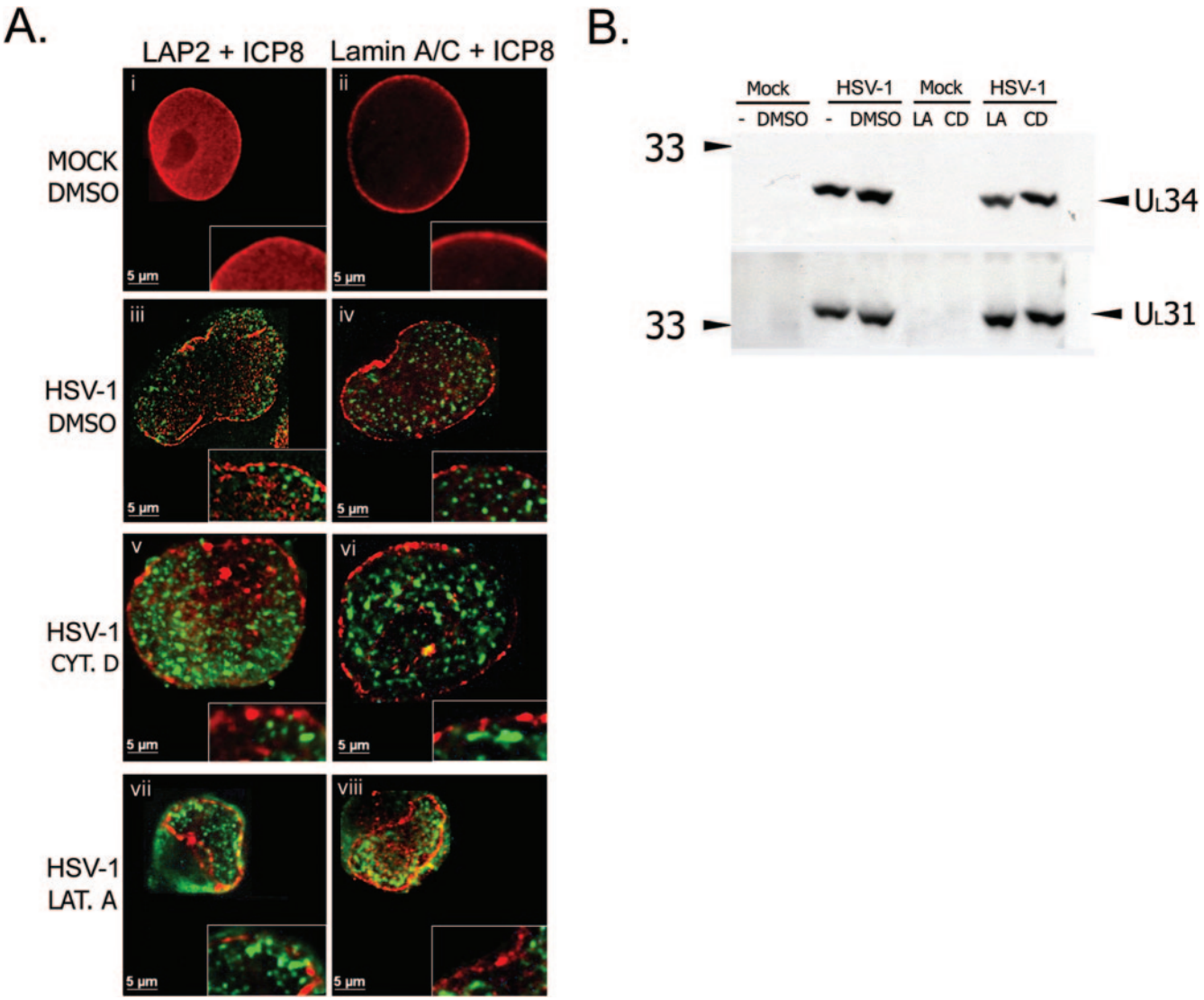


FIG. 5. Effects of latrunculin A and cytochalasin D during HSV-1 infection. (A) Digital images of fluorescence micrographs of HEp-2 cells mock infected (i and ii) or infected with wt HSV-1 (iii to viii) and treated with DMSO (i to iv), cytochalasin D (Cyt. D, v and vi), or latrunculin A (Lat. A, vii and viii). Cells were treated 2 hpi and were fixed 16 hpi and stained with antibodies to LAP2 and ICP8 (i, iii, v, and vii) or lamin A/C and ICP8 (ii, iv, vi, and viii). Merged-channel images are shown to show the relative localization of ICP8 and LAP2 or lamin A/C. Insets show digitally enlarged regions: enlargement is equal between images. (B) Western blots to detect UL31 and UL34. HEp-2 cells were infected with wt HSV-1 (HSV-1) or mock infected (Mock) and treated 2 hpi with DMSO, LA, or CD or were left untreated (−). Numbers at left are molecular mass in kilodaltons.

tion of monomeric G-actin by LA prevented nuclear expansion, chromatin fragmentation, and RC maturation while disruption of F-actin by CD had none of these effects.

**(ii) Disruption of G-actin does not prevent virus-induced lamina rearrangements.** Because G-actin disruption by LA prevented nuclear expansion and chromatin changes during infection with HSV-1, we determined if LA had any effect on disruption of the nuclear lamina seen during infection with wt HSV-1.

HEp-2 cells were infected with HSV-1 and treated from 2 hpi with LA, CD, or DMSO. At 16 hpi, cells were fixed and stained using antibodies to ICP8 and lamin A/C or LAP2. Mock-infected cells treated with DMSO (Fig. 5A, i and ii), CD, or LA (data not shown) showed smooth, continuous lamina staining. In the presence of DMSO in infected cells, RCs spread throughout the nucleus, and LAP2 staining was discontinuous and punctate at the nuclear rim (Fig. 5A, iii). The lamin A/C staining pattern was similarly discontinuous (Fig. 5A, iv). In the presence of CD the appearance of the lamina was similar to that in infected cells treated with DMSO (Fig. 5A, v and vi). In the presence of LA, nuclei were smaller than DMSO-treated cell nuclei, as described above (Fig. 4A, iii, and 4B and Fig. 5A, vii and viii). However, the lamina staining pattern appeared similar to that seen in DMSO-treated infected cells (Fig. 5A, iii, iv, vii, and viii). LAP2 and lamin A/C staining showed a discontinuous and punctate staining pattern at the nuclear edge. This pattern of lamina disruption was similar to that observed in CD- and DMSO-treated cells and to

TABLE 1. Viral yields from infections with different viral strains[a]

| Virus | Titer, 24 hpi (PFU/ml) |
|---|---|
| wt HSV-1 | $4.4 \times 10^7$ |
| dUL31 | $1.5 \times 10^5$ |
| dUL31R | $2.2 \times 10^6$ |
| dUL34 | $4.5 \times 10^3$ |
| dUL34R | $9.6 \times 10^5$ |

[a] Viral yields were measured following infection of HEp-2 cells with wt HSV-1, the viral mutant dUL31 or dUL34, or the rescued virus dUL31R or dUL34R. At 24 hpi, total infectivity was measured by plaque assay on Vero cells.

TABLE 2. Viral yields from infections in the presence of different inhibitors[a]

| Virus and treatment | Titer, 16 hpi (PFU/ml; avg, $n = 2$) |
|---|---|
| wt HSV-1, DMSO | $1.4 \times 10^6$ |
| wt HSV-1, CD | $2.1 \times 10^7$ |
| wt HSV-1, LA | $5.2 \times 10^6$ |

[a] Viral yield was measured following infection of HEp-2 cells with wt HSV-1 and treatment 2 hpi with DMSO, CD, or LA. At 16 hpi, total infectivity was measured by plaque assay on Vero cells.

that described previously in untreated cells (41). Thus, it appeared that G-actin function was not required for lamina disruption during HSV-1 infection.

**LA and CD treatment have no effect on UL31 and UL34 expression levels in infected cells.** Previous studies have shown that UL31 and UL34 are important in allowing changes in the nuclear architecture to occur during HSV-1 infection (41). Because our studies showed that G-actin might also be important in enabling a subset of these changes, we compared protein levels of UL31 and UL34 in treated and untreated cells. HEp-2 cells were infected with HSV-1 and treated from 2 hpi with DMSO, LA, or CD or were left untreated. At 16 hpi, cells were harvested, and SDS-PAGE and Western blotting were performed on the samples. In cells treated with DMSO, CD, or LA, levels of the UL31 and UL34 proteins were very similar to those detected in untreated cells (Fig. 5B). Therefore, cellular levels of the UL31 and UL34 proteins were unaffected by the presence of DMSO, LA, or CD.

**Deletion of the *UL31* or *UL34* ORFs causes a reduction in viral replication, whereas actin disruption by either CD or LA does not.** Mutant viruses defective for *UL31* or *UL34* exhibit replication defects, resulting in viral yields 1 to 2 $\log_{10}$ below those of rescued or wild-type viruses (35, 53). Because we saw the selective disruption of some of the nuclear changes ascribed to these proteins in the presence of LA, we determined the effects of LA and CD on viral replication.

HEp-2 cells were infected with dUL31, dUL34, the rescued virus dUL31R or dUL34R, or wt HSV-1. At 24 hpi, cells and supernatant were harvested together and total infectious virus was measured by plaque assay on Vero cells. The mutant virus dUL31 replicated to a titer 1 $\log_{10}$ lower than that of the rescued virus dUL31R (Table 1). The dUL34 virus replicated to 2 $\log_{10}$ lower than the corresponding rescued virus DUL34R. Thus, as previously observed, the deletion of either of these ORFs had a measurable effect on viral replication.

Treatment of HEp-2 cells infected with wt HSV-1 with LA or CD was done to compare the effect on replication with the deletion of the *UL31* or *UL34* gene. HEp-2 cells were infected with HSV-1 and then treated at 2 hpi with LA or CD or with DMSO as a solvent control. In contrast to the yields obtained in the absence of the *UL31* or *UL34* ORF, there was no decrease in titer following treatment with CD or LA compared to the DMSO-treated control (Table 2). These results were reproducible in multiple experiments (data not shown). There was a consistent increase of 1 $\log_{10}$ in the presence of CD. Thus, the disruption of actin by CD or LA had no negative effect on the ability of HSV-1 to replicate in HEp-2 cells. Thus, we conclude that actin disruption, to the extent described in these studies, did not prevent optimal HSV-1 replication, whereas deletion of *UL31* or *UL34* did decrease viral yield.

## DISCUSSION

HSV-1 infection has been shown to have a number of effects on the cell nucleus including marginalization of host chromatin (39), formation of RCs (32), nuclear enlargement (24), nuclear lamina disruption (41) or epitope masking (34), and chromatin dispersal (41). In this study we have shown that the nuclear lamina is disrupted during wild-type infection and that epitope masking does not account for the change in distribution of nuclear lamina proteins, through the use of a GFP-lamin A fusion protein. We also find that UL31 and UL34 proteins are essential for nuclear expansion during infection. HSV-1 disrupts a nuclear skeleton as revealed by the redistribution of the GFP-Cdc14B protein. G-actin is essential for the increase in nuclear size control during infection. The use of various actin inhibitors and viral mutants allowed the distinction of some of these nuclear modifications in the context of viral replication. From these studies it appears that lamina disruption is required to achieve wild-type levels of viral replication, while nuclear expansion and chromatin dispersal appear to be dispensable in this regard.

**Control of nuclear size.** In uninfected cells, nuclear size is linked to the cell cycle and can increase threefold during S phase (52). Mutant forms of BRG1, the catalytic core subunit of the SWI/SNF chromatin remodeling enzymes, when expressed in cultured cells, cause an increase of 10% in nuclear cross-sectional area. In contrast to HSV-1 infection, no changes in chromatin localization are observed under these conditions (12). Thus, factors involved in the control of nuclear size in uninfected cells appear to include chromatin structure and DNA replication and may also include the nucleoskeleton (26). In addition, overexpression of the lamin-binding fragment of LAP2 has been found to inhibit nuclear size increases during S phase in uninfected cells (52), implying that lamina dynamics also play a role in the control of nuclear size. During HSV-1 infection, we find that disruption of the nuclear lamina may be necessary but is not sufficient for nuclear expansion, because during LA treatment, infected nuclei show lamina disruption but do not expand. We have found no example in the cell biological literature of nuclear expansion of the magnitude seen here during HSV-1 infection. We find that nuclear cross-sectional area doubles, reflecting an increase in volume of four- to fivefold. In preliminary experiments in which nuclear volume was calculated, we found an increase of almost

fivefold in infected cells at 16 hpi compared to mock-infected cells (data not shown).

**Role of G-actin.** G-actin has been postulated to have nuclear functions in uninfected cells (31). Our results indicate that G-actin is essential for nuclear enlargement during HSV infection. We find that, in the presence of LA, which binds to and sequesters G-actin monomers, several nuclear changes associated with HSV-1 infection are inhibited: nuclear size does not increase, RCs do not mature, and chromatin is not dispersed. In contrast, as mentioned above, the lamina is disrupted during infection in the presence of LA. CD, which specifically binds to the growing ends of F-actin filaments and prevents polymerization, has none of these inhibitory effects on changes to the nuclear architecture during infection. Thus, G-actin appears to be involved in nuclear expansion during HSV-1 infection, and the sequestration of G-actin monomers during LA treatment prevents this from occurring. It is therefore possible that G-actin forms part of a nuclear size control mechanism in uninfected cells. Although we postulate that this novel G-actin function might be performed by nuclear G-actin, it is possible that cytoplasmic G-actin is responsible: unfortunately, no commercial reagents are currently available to distinguish between these possibilities. Such a function would be consistent with suggested roles for nuclear actin in nuclear architecture (13, 31). The fact that LA treatment inhibits RC maturation and chromatin dispersal in addition to nuclear expansion leads us to speculate that RC maturation is one cause of nuclear expansion and that this involves G-actin. However, it is also possible that the mechanism of chromatin marginalization and nuclear expansion is not driven by mechanical forces but by changes in host cell gene expression. Lamina disruption appears to occur independently of RC maturation and G-actin function and requires expression of the viral UL31 and UL34 proteins.

In uninfected cells, changes in overall cell size and shape are reflected by proportionate changes in nuclear size and shape (4, 16, 43). Cell spreading and attachment to a culture surface are required for DNA replication, and hence nuclear expansion, in cultured cells (4, 14, 15, 17, 42). During HSV-1 infection, in contrast to events in uninfected cells, dramatic nuclear expansion and changes in nuclear shape are concurrent with overall cell rounding and detachment from the culture surface; thus, the two properties are no longer synchronous. The fact that variation in nuclear size increases during infection with HSV-1 implies that some cells resist changes in nuclear size more than others. This may reflect differing mechanical forces across the monolayer (14) or may be the result of variation in the viral load or infection dynamics from cell to cell. In either case, HSV-1-infected cells behave differently from uninfected cells, in which cell rounding is reflected by proportionate rounding and contraction of nuclei (4, 16, 43). This suggests that a cellular mechanism for the control of nuclear shape and size exists and that HSV-1 infection disrupts this mechanism, allowing nuclear expansion outside normal cellular limits.

Nuclear shape is linked to the structure of the lamina (27). In granulocytes, during formation of the distinctive lobular nucleus, the proposed mechanism involves thinning of the lamina to make the nuclear membrane more flexible, in conjunction with increased lamin B receptor expression, increased interactions with chromatin, and forces exerted by the cytoskeleton, which pull the nucleus into shape (28). Additionally, in cells from mice lacking the lamin A gene, nuclei are misshapen and heterochromatin is mislocalized (27). The data shown here following HSV-1 infection, during which nuclei expand and nuclear shape is altered concurrent with lamina disruption, are consistent with these observations. Thus, the lamina disruption recorded here may be partly responsible for nuclear size increases during HSV-1 infection. The dramatic changes in chromatin localization may also be due in part to lamina disruption (e.g., Fig. 1). As mentioned above, however, lamina disruption may be necessary but is not sufficient for chromatin dispersal in infected cells, because LA treatment does not prevent lamina disruption but does prevent RC maturation and chromatin disruption.

**Nuclear changes and viral replication.** No decrease in viral yield was observed following treatment of infected cells with LA or CD. Therefore, despite the dramatic changes in nuclear size, RC maturation, and the dispersal of host chromatin, these processes appear to be dispensable for viral replication. By contrast, the DUL31 and DUL34 mutant viruses consistently show reduced viral yields in our system. Thus, we find that lamina disruption appears to be required for maximal viral replication in vitro. It is, however, of note that the deletion mutant viruses DUL31 and DUL34 are able to replicate to some degree in noncomplementing cell lines, indicating that nuclear egress can occur even in the absence of the changes in nuclear architecture caused by these proteins (3, 38).

The role of lamina disruption caused by UL31 and UL34 during viral replication may be to facilitate nuclear egress. HSV-1 nucleocapsids are thought to exit the nucleus by budding at the inner nuclear membrane; therefore, access to this membrane might be increased by lamina disruption (41). It has also been suggested that the UL31 and UL34 complex, which is located in the inner nuclear membrane, might act as a docking site for nucleocapsids, promoting budding (34). An alternative strategy for nuclear egress of herpesviruses has recently been suggested, via exit through large, impaired nuclear pore structures (50). Nuclear pore complexes are highly organized, regular structures which selectively control the trafficking of molecules between the nucleus and cytoplasm (33). It has been observed in bovine herpesvirus 1-infected cells that nuclei have large gaps in their membranes during infection, through which nucleocapsids may exit the nucleus (50), sidestepping the traditional egress pathway, which requires that they bud through the inner nuclear membrane to be released into the cytoplasm by fusion at the outer nuclear membrane (2, 11, 49). The findings presented here do not distinguish between the suggested pathways for nuclear egress. Lamina disruption does appear to promote egress, and this step could be incorporated into any of the proposed models for egress. The fact that mutants lacking *UL31* or *UL34* are able to replicate to within 1 to 2 $\log_{10}$ of wild-type and rescued viruses supports the hypothesis that there is a UL31/UL34-independent route out of the nucleus; thus, there might be more than one mechanism of egress. Lamina disruption may both promote access of capsids to the inner nuclear membrane and also destabilize the membrane to some degree, possibly allowing nuclear pores to be disrupted. Such impairment of nuclear pore complexes has also been proposed to account for nuclear expansion during bovine herpesvirus 1 infection; however, nuclei were found to

expand far less than those observed here during HSV-1 infection (50). Further studies are required to address these different mechanisms for nuclear egress during herpesvirus infection.

HSV-1 has been proposed to undergo an assembly step in nuclear compartments termed assemblons, which are visible by staining for capsid proteins during the later stages of infection (47). Indeed, movement of GFP-tagged viral nucleocapsids away from such structures has recently been reported to be inhibited selectively by LA, implying a possible role for G-actin in intranuclear movement during infection (7). The dose of LA used in that study (4.7 μM) is more than four times that used here to show defects in nuclear maturation during infection (1 μM); thus, direct comparisons in terms of impact on viral yields cannot be made. However, in multiple experiments we find no decrease in viral yield using LA up to 2.5 μM (data not shown). Therefore, a role for actin-based nuclear movement of capsids in viral replication has yet to be established. Although we do see aggregates of capsid protein in a small percentage of cells, we find that the majority of cells in 16-h infection experiments do not contain assemblons. Therefore, it is possible that these structures are not required for replication. It is, however, also feasible that nucleocapsids are assembled in small foci not easily visible by light microscopy.

In conclusion, we have described nuclear expansion, lamina disruption, and chromatin dispersal during HSV-1 infection and have defined the importance of these processes during replication. We have shown that G-actin is essential for nuclear expansion during HSV-1 infection. We have confirmed the involvement of the UL31 and UL34 viral proteins in lamina disruption and have identified a novel role for these proteins in nuclear expansion. In addition, we show the first evidence that the nucleoskeleton is disrupted by HSV-1. We find that nuclear expansion and chromatin dispersal are dispensable for viral replication. In contrast, lamina disruption correlates with optimal levels of viral replication. Further investigation of the nature of the disruption of the nuclear lamina during HSV-1 infection will lead to greater insights regarding the mechanism(s) of nuclear egress in herpesviruses.

## ACKNOWLEDGMENTS

We thank Bernard Roizman for the gift of the R5132 and R5133 viruses, Richard Roller for the gift of the RR1072 and RR1072R viruses and antiserum to UL34, Joel Baines for the gift of antiserum to UL31, and David Gilbert for the gift of plasmid pGFPWTLA.

This research was supported by NIH grants AI063106 (D.M.K.) and GM54137 (J.W.H.).

## REFERENCES

1. **Bettinger, B. T., D. M. Gilbert, and D. C. Amberg.** 2004. Actin up in the nucleus. Nat. Rev. Mol. Cell Biol. **5:**410–415.
2. **Browne, H., S. Bell, T. Minson, and D. W. Wilson.** 1996. An endoplasmic reticulum-retained herpes simplex virus glycoprotein H is absent from secreted virions: evidence for reenvelopment during egress. J. Virol. **70:**4311–4316.
3. **Chang, Y. E., and B. Roizman.** 1993. The product of the $U_L31$ gene of herpes simplex virus 1 is a nuclear phosphoprotein which partitions with the nuclear matrix. J. Virol. **67:**6348–6356.
4. **Couchman, J. R., D. A. Rees, M. R. Green, and C. G. Smith.** 1982. Fibronectin has a dual role in locomotion and anchorage of primary chick fibroblasts and can promote entry into the division cycle. J. Cell Biol. **93:**402–410.
5. **Dreger, C. K., A. R. Konig, H. Spring, P. Lichter, and H. Herrmann.** 2002. Investigation of nuclear architecture with a domain-presenting expression system. J. Struct. Biol. **140:**100–115.
6. **Farina, A., R. Feederle, S. Raffa, R. Gonnella, R. Santarelli, L. Frati, A. Angeloni, M. R. Torrisi, A. Faggioni, and H. J. Delecluse.** 2005. BFRF1 of Epstein-Barr virus is essential for efficient primary viral envelopment and egress. J. Virol. **79:**3703–3712.
7. **Forest, T., S. Barnard, and J. D. Baines.** 2005. Active intranuclear movement of herpesvirus capsids. Nat. Cell Biol. **7:**429–431.
8. **Fuchs, W., B. G. Klupp, H. Granzow, N. Osterrieder, and T. C. Mettenleiter.** 2002. The interacting UL31 and UL34 gene products of pseudorabies virus are involved in egress from the host-cell nucleus and represent components of primary enveloped but not mature virions. J. Virol. **76:**364–378.
9. **Gonnella, R., A. Farina, R. Santarelli, S. Raffa, R. Feederle, R. Bei, M. Granato, A. Modesti, L. Frati, H. J. Delecluse, M. R. Torrisi, A. Angeloni, and A. Faggioni.** 2005. Characterization and intracellular localization of the Epstein-Barr virus protein BFLF2: interactions with BFRF1 and with the nuclear lamina. J. Virol. **79:**3713–3727.
10. **Gonsior, S. M., S. Platz, S. Buchmeier, U. Scheer, B. M. Jockusch, and H. Hinssen.** 1999. Conformational difference between nuclear and cytoplasmic actin as detected by a monoclonal antibody. J. Cell Sci. **112:**797–809.
11. **Granzow, H., B. G. Klupp, W. Fuchs, J. Veits, N. Osterrieder, and T. C. Mettenleiter.** 2001. Egress of alphaherpesviruses: comparative ultrastructural study. J. Virol. **75:**3675–3684.
12. **Hill, D. A., S. Chiosea, S. Jamaluddin, K. Roy, A. H. Fischer, D. D. Boyd, J. A. Nickerson, and A. N. Imbalzano.** 2004. Inducible changes in cell size and attachment area due to expression of a mutant SWI/SNF chromatin remodeling enzyme. J. Cell Sci. **117:**5847–5854.
13. **Holaska, J. M., A. K. Kowalski, and K. L. Wilson.** 2004. Emerin caps the pointed end of actin filaments: evidence for an actin cortical network at the nuclear inner membrane. PLoS Biol. **2:**E231.
14. **Ingber, D. E.** 1993. Cellular tensegrity: defining new rules of biological design that govern the cytoskeleton. J. Cell Sci. **104:**613–627.
15. **Ingber, D. E.** 1990. Fibronectin controls capillary endothelial cell growth by modulating cell shape. Proc. Natl. Acad. Sci. USA **87:**3579–3583.
16. **Ingber, D. E.** 2003. Tensegrity I. Cell structure and hierarchical systems biology. J. Cell Sci. **116:**1157–1173.
17. **Ingber, D. E., J. A. Madri, and J. Folkman.** 1987. Endothelial growth factors and extracellular matrix regulate DNA synthesis through modulation of cell and nuclear expansion. In Vitro Cell Dev. Biol. **23:**387–394.
18. **Izumi, M., O. A. Vaughan, C. J. Hutchison, and D. M. Gilbert.** 2000. Head and/or CaaX domain deletions of lamin proteins disrupt preformed lamin A and C but not lamin B structure in mammalian cells. Mol. Biol. Cell **11:**4323–4337.
19. **Klupp, B. G., H. Granzow, and T. C. Mettenleiter.** 2000. Primary envelopment of pseudorabies virus at the nuclear membrane requires the UL34 gene product. J. Virol. **74:**10063–10073.
20. **Knipe, D. M., D. Senechek, S. A. Rice, and J. L. Smith.** 1987. Stages in the nuclear association of the herpes simplex virus transcriptional activator protein ICP4. J. Virol. **61:**276–284.
21. **Lake, C. M., and L. M. Hutt-Fletcher.** 2004. The Epstein-Barr virus BFRF1 and BFLF2 proteins interact and coexpression alters their cellular localization. Virology **320:**99–106.
22. **Liang, L., and J. D. Baines.** 2005. Identification of an essential domain in the herpes simplex virus 1 UL34 protein that is necessary and sufficient to interact with UL31 protein. J. Virol. **79:**3797–3806.
23. **Martelli, A. M., E. Falcieri, M. Zweyer, R. Bortul, G. Tabellini, A. Cappellini, L. Cocco, and L. Manzoli.** 2002. The controversial nuclear matrix: a balanced point of view. Histol. Histopathol. **17:**1193–1205.
24. **Monier, K., J. C. Armas, S. Etteldorf, P. Ghazal, and K. F. Sullivan.** 2000. Annexation of the interchromosomal space during viral infection. Nat. Cell Biol. **2:**661–665.
25. **Muranyi, W., J. Haas, M. Wagner, G. Krohne, and U. H. Koszinowski.** 2002. Cytomegalovirus recruitment of cellular kinases to dissolve the nuclear lamina. Science **297:**854–857.
26. **Nalepa, G., and J. W. Harper.** 2004. Visualization of a highly organized intranuclear network of filaments in living mammalian cells. Cell Motil. Cytoskelet. **59:**94–108.
27. **Nikolova, V., C. Leimena, A. C. McMahon, J. C. Tan, S. Chandar, D. Jogia, S. H. Kesteven, J. Michalicek, R. Otway, F. Verheyen, S. Rainer, C. L. Stewart, D. Martin, M. P. Feneley, and D. Fatkin.** 2004. Defects in nuclear structure and function promote dilated cardiomyopathy in lamin A/C-deficient mice. J. Clin. Investig. **113:**357–369.
28. **Olins, A. L., and D. E. Olins.** 2004. Cytoskeletal influences on nuclear shape in granulocytic HL-60 cells. BMC Cell Biol. **5:**30.
29. **Pederson, T.** 2000. Diffusional protein transport within the nucleus: a message in the medium. Nat. Cell Biol. **2:**E73–E74.
30. **Pederson, T.** 2000. Half a century of "the nuclear matrix." Mol. Biol. Cell **11:**799–805.
31. **Pederson, T., and U. Aebi.** 2002. Actin in the nucleus: what form and what for? J. Struct. Biol. **140:**3–9.
32. **Quinlan, M. P., L. B. Chen, and D. M. Knipe.** 1984. The intranuclear location of a herpes simplex virus DNA-binding protein is determined by the status of viral DNA replication. Cell **36:**857–868.
33. **Rabut, G., V. Doye, and J. Ellenberg.** 2004. Mapping the dynamic organiza-

tion of the nuclear pore complex inside single living cells. Nat. Cell Biol. **6:**1114–1121.
34. **Reynolds, A. E., L. Liang, and J. D. Baines.** 2004. Conformational changes in the nuclear lamina induced by herpes simplex virus type 1 require genes $U_L31$ and $U_L34$. J. Virol. **78:**5564–5575.
35. **Reynolds, A. E., B. J. Ryckman, J. D. Baines, Y. Zhou, L. Liang, and R. J. Roller.** 2001. $U_L31$ and $U_L34$ proteins of herpes simplex virus type 1 form a complex that accumulates at the nuclear rim and is required for envelopment of nucleocapsids. J. Virol. **75:**8803–8817.
36. **Reynolds, A. E., E. G. Wills, R. J. Roller, B. J. Ryckman, and J. D. Baines.** 2002. Ultrastructural localization of the herpes simplex virus type 1 $U_L31$, $U_L34$, and $U_S3$ proteins suggests specific roles in primary envelopment and egress of nucleocapsids. J. Virol. **76:**8939–8952.
37. **Roizman, B., and D. M. Knipe.** 2001. Herpes simplex viruses and their replication, p. 2399–2460. *In* D. M. Knipe and P. M. Howley (ed.), Fields virology, 4th ed. Lippincott Williams & Wilkins, Philadelphia, Pa.
38. **Roller, R. J., Y. Zhou, R. Schnetzer, J. Ferguson, and D. DeSalvo.** 2000. Herpes simplex virus type 1 $U_L34$ gene product is required for viral envelopment. J. Virol. **74:**117–129.
39. **Schwartz, J., and B. Roizman.** 1969. Concerning the egress of herpes simplex virus from infected cells: electron and light microscope observations. Virology **38:**42–49.
40. **Scott, E. S., and P. O'Hare.** 2001. Fate of the inner nuclear membrane protein lamin B receptor and nuclear lamins in herpes simplex virus type 1 infection. J. Virol. **75:**8818–8830.
41. **Simpson-Holley, M., J. Baines, R. Roller, and D. M. Knipe.** 2004. Herpes simplex virus 1 *$U_L31$* and *$U_L34$* gene products promote the late maturation of viral replication compartments to the nuclear periphery. J. Virol. **78:**5591–5600.
42. **Sims, J. R., S. Karp, and D. E. Ingber.** 1992. Altering the cellular mechanical force balance results in integrated changes in cell, cytoskeletal and nuclear shape. J. Cell Sci. **103:**1215–1222.
43. **Swanson, J. A., M. Lee, and P. E. Knapp.** 1991. Cellular dimensions affecting the nucleocytoplasmic volume ratio. J. Cell Biol. **115:**941–948.
44. **Taylor, T. J., E. E. McNamee, C. Day, and D. M. Knipe.** 2003. Herpes simplex virus replication compartments can form by coalescence of smaller compartments. Virology **309:**232–247.
45. **Uprichard, S. L., and D. M. Knipe.** 1997. Assembly of herpes simplex virus replication proteins at two distinct intranuclear sites. Virology **229:**113–125.
46. **Visintin, R., K. Craig, E. S. Hwang, S. Prinz, M. Tyers, and A. Amon.** 1998. The phosphatase Cdc14 triggers mitotic exit by reversal of Cdk-dependent phosphorylation. Mol. Cell **2:**709–718.
47. **Ward, P. L., W. O. Ogle, and B. Roizman.** 1996. Assemblons: nuclear structures defined by aggregation of immature capsids and some tegument proteins of herpes simplex virus 1. J. Virol. **70:**4623–4631.
48. **Wasser, M., and W. Chia.** 2000. The EAST protein of drosophila controls an expandable nuclear endoskeleton. Nat. Cell Biol. **2:**268–275.
49. **Whealy, M. E., A. K. Robbins, F. Tufaro, and L. W. Enquist.** 1992. A cellular function is required for pseudorabies virus envelope glycoprotein processing and virus egress. J. Virol. **66:**3803–3810.
50. **Wild, P., M. Engels, C. Senn, K. Tobler, U. Ziegler, E. M. Schraner, E. Loepfe, M. Ackermann, M. Mueller, and P. Walther.** 2005. Impairment of nuclear pores in bovine herpesvirus 1-infected MDBK cells. J. Virol. **79:**1071–1083.
51. **Yamauchi, Y., C. Shiba, F. Goshima, A. Nawa, T. Murata, and Y. Nishiyama.** 2001. Herpes simplex virus type 2 UL34 protein requires UL31 protein for its relocation to the internal nuclear membrane in transfected cells. J. Gen. Virol. **82:**1423–1428.
52. **Yang, L., T. Guan, and L. Gerace.** 1997. Lamin-binding fragment of LAP2 inhibits increase in nuclear volume during the cell cycle and progression into S phase. J. Cell Biol. **139:**1077–1087.
53. **Ye, G. J., and B. Roizman.** 2000. The essential protein encoded by the UL31 gene of herpes simplex virus 1 depends for its stability on the presence of UL34 protein. Proc. Natl. Acad. Sci. USA **97:**11002–11007.